Electronic Supplementary information of **Thermal transport across nanoparticle-fluid interfaces: the interplay of interfacial curvature and nanoparticle-fluid interactions**

Anna Sofia Tascini[a], Jeff Armstrong[a,b], Eliodoro Chiavazzo[c], Matteo Fasano[c], Pietro Asinari[c] and Fernando Bresme*[,a]

1 Temperature profiles

1.1 Cut-off effect

Since employing a different cutoff can give slightly different coexistence properties and transport coefficients, we computed the temperature profiles around the nanoparticles for two different cut-off radii (R_c= 2.5 and 4.4) in the case of three different fluid-nanoparticle interaction strengths (F=0.1, 0.5 and 1.0). Fig. S1 shows that the differences in the two cases are negligible. Therefore we can assume that the general physical behaviour explored in this study (where R_c= 2.5) remains the same.

1.2 Solving the heat diffusion equation

We fitted our simulated temperature profiles to the solution of the one dimensional heat diffusion equation under stationary conditions. To simplify the modelling approach we assumed that the thermal conductivities of the nanoparticle and the fluid are constant and independent of the radial distance to the nanoparticle centre of mass. The temperature profiles from MD simulations were fitted to Fourier's law of heat conduction, which at the steady state is given by $T(r) = \frac{A}{r} + B$, where A and B are constants that can be calculated by considering the boundary conditions of the heat diffusion equation.

We consider the heat diffusion equation in spherical coordinates. This significantly simplifies the equations we need to solve, since the problem is one dimensional. The heat diffusion equation can then be written as:

$$\frac{Q}{4\pi r^2} = -\lambda_\alpha \frac{dT}{dr},$$

where Q is the heat transferred, $4\pi r^2$ is the corresponding isothermal area and λ_α is the thermal conductivity of phase α (nanoparticle or liquid).

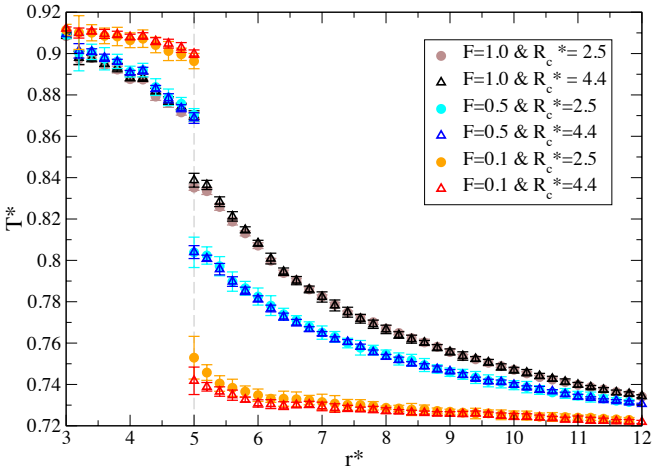

Fig. S1 Temperature profiles of nanoparticles of radius 5 and different fluid-nanoparticle interaction strengths. Results for two cut-offs, 2.5 and 4 are shown.

We solve the differential equation (using Dirichlet boundary conditions) between radius r_1 at temperature $T = T_1$ and radius r at temperature T:

$$\frac{-Q}{4\pi}\int_{r_1}^{r}\frac{1}{r^2}dr = \lambda_\alpha \int_{T_1}^{T} dT,$$

The temperature profile is then defined by:

$$T(r) = \frac{Q}{4\pi\lambda_\alpha}\left(\frac{1}{r} - \frac{1}{r_1}\right) + T_1 \;\approx\; T(r) = \frac{A}{r} + B.$$

The fitting of the simulated temperature profiles to the equation above gives estimates of the fluid and nanoparticle thermal conductivities. The latter follow directly from the integration con-

[a] *Department of Chemistry, Imperial College London, SW7 2AZ, UK*
[b] *ISIS Facility, Rutherford Appleton Laboratory, Chilton, Didcot, Oxfordshire, OX11 0QX, UK*
[c] *Department of Energy, Politecnico di Torino, 10129, Torino, Italy*
† email:anna.tascini13@imperial.ac.uk;f.bresme@imperial.ac.uk

stant, A, corresponding to the best fit:

$$\lambda_\alpha = \frac{Q}{4\pi A}.$$

In addition we solved the heat diffusion equation numerically, using a second order central finite difference method (FD) [1,2]. In this way, we can consider in the solution the effect of the thermal boundary resistance at the interface ($r^* = R^*$). Fourier's law in spherical coordinates (reduced to the one dimensional case) at the steady state can be written as follows:

$$-\frac{1}{r^2}\frac{\partial}{\partial r}\left(\lambda_\alpha r^2 \frac{\partial T}{\partial r}\right) = 0,$$

and simplified to:

$$-\lambda_\alpha \frac{\partial^2 T}{\partial r^2} - \frac{2\lambda_\alpha}{r}\frac{\partial T}{\partial r} = 0.$$

Following the FD method we perform a discretisation of the spatial domain in n nodes, using an homogeneous mesh (Δr). At node i the previous equation can be reformulated as:

$$-\lambda_\alpha \frac{T_{i+1} - 2T_i + T_{i-1}}{\Delta r^2} - \frac{2\lambda_\alpha}{r_i}\frac{T_{i+1} - T_{i-1}}{2\Delta r} = 0.$$

and rearranged as follows:

$$T_{i+1}\left[-\frac{\lambda_\alpha}{\Delta r}\left(\frac{1}{\Delta r} + \frac{1}{r_i}\right)\right] + T_i\left[\frac{2\lambda_\alpha}{\Delta r^2}\right] + T_{i-1}\left[-\frac{\lambda_\alpha}{\Delta r}\left(\frac{1}{\Delta r} - \frac{1}{r_i}\right)\right] = 0 \quad (1)$$

The resulting system of n equations can be solved considering a linear system:

$$[A]\,\mathbf{T} = \mathbf{b}.$$

Where: $[A](\lambda_{NP}, \lambda_L, G_K)$ is a tridiagonal matrix, defined according to equation (1), which includes: a constant term equal to $\left[2\frac{\lambda_\alpha}{\Delta r^2}\right]$ along the main diagonal of the matrix, an r-dependent term equal to $\left[-\frac{\lambda_\alpha}{\Delta r}\left(\frac{1}{\Delta r} + \frac{1}{r_i}\right)\right]$ along the first diagonal above the main one, and an r-dependent term equal to $\left[-\frac{\lambda_\alpha}{\Delta r}\left(\frac{1}{\Delta r} - \frac{1}{r_i}\right)\right]$ along the first diagonal below. The application of the FD procedure requires the modification of the row *1*, *k*, *k+1* (where k indicates the node i corresponding to the nanoparticle interface and $k+1$ the fluid one) and n to take into account the boundary conditions of the problem (see below); the vector $\mathbf{T}$ defines the temperature distribution along the radial distance r, and $\mathbf{b}$ is a vector where all the elements are zero, except the first $\mathbf{b}[1]$ and last $\mathbf{b}[n]$ elements, which define the boundary conditions of the problems at $r^* = r_H$ and $r^* = r_C$, respectively (as described below).

$r^* = r_H$ and $r^* = r_C$ denote the radial distances corresponding to the hot and cold thermostats. At the first node ($i = 1$ and $r^* = r_H$) and the last node ($i = n$ and $r^* = r_C$) the thermostatting process is described via *Dirichlet* boundary conditions, which results in the following conditions:

$$b(1) = T_H,\ A(1,1) = 1,\ A(1,2) = 0$$

$$b(n) = T_C,\ A(n,n) = 1,\ A(n,n-1) = 0$$

Robin boundary conditions are used to model the heat transport at the interface ($r^* = R^*$), and to take into account the temperature drop (ΔT) due to the thermal boundary conductance at the interface:

$$-\lambda\frac{\partial T}{\partial r} = G_K \Delta T. \quad (2)$$

This equation has to be included in the definition of the tridiagonal matrix $[A]$ in the three values of the two rows corresponding to the nanoparticle-fluid interface (here k and $k+1$):

$$\begin{aligned} A(k,k-1) &= \frac{\lambda_{NP}}{\Delta r} - G_K, \\ A(k,k) &= -\frac{\lambda_{NP}}{\Delta r}, \\ A(k,k+1) &= G_K; \\ \\ A(k+1,k) &= -G_K, \\ A(k+1,k+1) &= \frac{\lambda_L}{\Delta r}, \\ A(k+1,k+2) &= -\frac{\lambda_L}{\Delta r} + G_K. \end{aligned}$$

where k indicates the node i corresponding to the nanoparticle interface ($r^* = R^*$), whilst $k+1$ the fluid ones, at $r^* = R^* + \Delta r$.

The solution of the linear system gives the temperature profile, $\mathbf{T} = [A]^{-1}\,\mathbf{b}$, at each node along the radial distance.

To calculate the transport coefficients (λ_{NP}, λ_L and G_K) we minimised (with a threshold of 10^{-5}) the mean squared error between the temperature profiles obtained in the MD simulations and the ones predicted by the FD scheme. The temperature profiles obtained from the FD approach are shown in Fig. 5(in the main paper), and estimates of the thermal conductivities and thermal conductances are given in Tables S1 and S2 below.

Fig. S2 shows the thermal conductivities obtained from the FD approach as a function of the interaction parameter F.

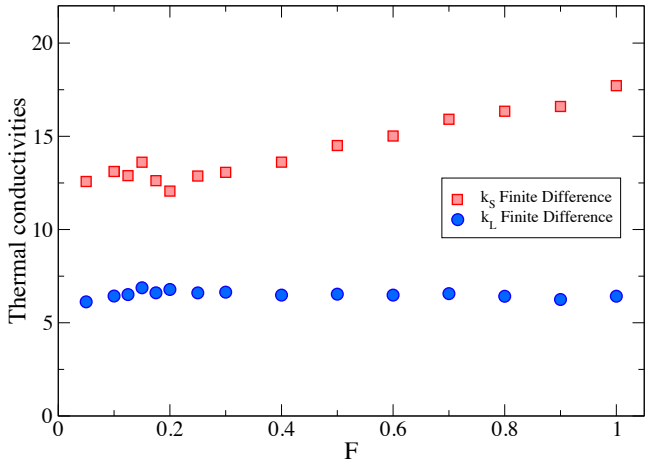

Fig. S2 The thermal conductivities of the nanoparticle and the fluid evaluated using the FD approach.

2 Velocity Autocorrelation Functions and Power Spectra

To compute the interfacial contributions to the velocity autocorrelation function we defined two regions. One, for the interfacial fluid monolayer, which includes all the atoms inside a spherical shell of radius, $r^* = 6.2$, around the nanoparticle. The second region is defined relative to the particle corona, and includes all the nanoparticle atoms outside a spherical shell of radius $r^* = 4.5$. The maximum correlation time for the velocity autocorrelation function was $t_{max}* = 5$ (corresponding to 5000 time steps). Only those particles that remained in the shells defined above, during the entire sampling time, *i.e*, from $t_0 = 0$ to $t_{max} = 5$, where included in the analysis of the interfacial contributions. Particles outside these layers were employed to compute the “bulk" contributions for the nanoparticle and the fluid.

The power spectrum was computed by discretising the velocity autocorrelation function in the frequency domain. We used the MATLAB library *fft*. The sampling frequency was $F_S^* = 1/t^* = 1000$ (in reduced units).

TABLES

Tables S1 and S2 contains all the data discussed in the main paper in reduced and real units, respectively, are reported below.

References

1 C. Johnson, *Numerical solution of partial differential equations by the finite element method*, 1987, vol. 32, p. 278.

2 J. Peiro and S. Sherwin, *Handbook of Materials Modeling*, Springer Netherlands, Dordrecht, 2005, pp. 2415–2446.

	MD		FD		
F	G_k^*	δG_K^*	λ_{NP}^*	G_K^*	λ_L^*
0.05 •	0.126	0.004	12.577	0.148	6.121
0.1 •	0.250	0.009	13.116	0.275	6.434
0.125	0.303	0.008	12.891	0.330	6.513
0.15 •	0.370	0.011	13.611	0.348	6.877
0.175	0.459	0.013	12.623	0.494	6.605
0.2 •	0.561	0.015	12.061	0.599	6.785
0.25	0.740	0.028	12.871	0.760	6.603
0.3 •	0.941	0.039	13.068	1.007	6.640
0.4 •	1.426	0.052	13.613	1.447	6.484
0.5 •	1.965	0.079	14.508	1.938	6.535
0.6 •	2.472	0.151	15.016	2.403	6.482
0.7	3.227	0.178	15.916	3.070	6.563
0.8 •	3.725	0.373	16.347	3.553	6.420
0.9	4.440	0.256	16.600	4.090	6.248
1.0 •	5.571	0.569	17.717	4.737	6.423

Table S1 Thermal conductances, G_K^*, and thermal conductivities, λ_α^* (α=NP – nanoparticle, L – liquid) of the nanoparticle and liquid as a function of the interaction strength, F. All the data correspond to a nanoparticle of radius $R^* = 5$. δG_K represents the uncertainty of the thermal conductance. The bullet points indicate the systems represented in Fig. 5 and 7-(Top).

	MD		FD		
F	G_K $[MWm^{-2}K^{-1}]$	δG_K $[MWm^{-2}K^{-1}]$	λ_{NP} $[Wm^{-1}K^{-1}]$	G_K $[MWm^{-2}K^{-1}]$	λ_L $[Wm^{-1}K^{-1}]$
0.05	7.032	0.206	0.238	8.241	0.116
0.1	13.93	0.474	0.249	15.30	0.122
0.125	16.88	0.429	0.244	18.38	0.123
0.15	20.63	0.602	0.258	19.41	0.130
0.175	25.57	0.708	0.239	27.55	0.125
0.2	31.25	0.841	0.229	33.36	0.129
0.3	52.45	2.190	0.248	56.11	0.126
0.4	79.48	2.903	0.258	80.63	0.123
0.5	109.5	4.408	0.275	108.0	0.124
0.6	137.8	8.414	0.285	133.9	0.123
0.7	179.8	9.936	0.301	171.1	0.124
0.8	207.6	20.76	0.310	197.9	0.122
0.9	247.4	14.288	0.314	227.9	0.118
1.0	310.5	31.72	0.336	264.0	0.122

Table S2 Same as Table 2 but in SI units. We used $\sigma = 3.405$ Å and $\varepsilon = 0.996$ kJ/mol for the conversion from reduced to SI units.